J. Physiol. (1980), **305**, *pp.* 377–395
With 11 *text-figures*
Printed in Great Britain

CONTROL OF REPETITIVE FIRING IN SQUID AXON MEMBRANE AS A MODEL FOR A NEURONEOSCILLATOR

BY RITA GUTTMAN, STEPHEN LEWIS AND JOHN RINZEL*

From the Department of Biology,
Brooklyn College of the City University of New York, Brooklyn, New York 11210,
the Marine Biological Laboratory, Woods Hole, Massachussetts, 02543 and
the Mathematical Research Branch, NIAMDD, N.I.H.
Bethesda, Maryland, 20205, U.S.A.*

(*Received 16 January 1979*)

SUMMARY

1. Repetitive firing in space-clamped squid axons bathed in low Ca and stimulated by a just suprathreshold step of current can be annihilated by a brief depolarizing or hyperpolarizing pulse of the proper magnitude applied at the proper phase.

2. In response to such perturbations, membrane potential and ionic currents show damped oscillations toward a steady state.

3. For other, non-annihilating, perturbations repetitive firing resumes with unaltered frequency but with phase resetting.

4. Experimental findings are compared with calculations for the space- and current-clamped Hodgkin–Huxley equations. Annihilation of repetitive firing to a steady state corresponds to a solution trajectory perturbed off a stable limit cycle and into the domain of attraction of a coexistent stable singular point.

5. Experimentally and theoretically the nerve exhibits hysteresis with two different stable modes of operation for a just suprathreshold range of bias current: the oscillatory repetitive firing state and the time-independent steady state.

6. Analogy is made to a brief synaptic input (excitatory or inhibitory) which may start or stop a biological pace-maker.

INTRODUCTION

The finding that biological membranes can exhibit properties akin to that of an inductive reactance, which allows for an analogous equivalent membrane circuit that is oscillatory (Cole & Baker, 1941) was crucial in establishing a theoretical underpinning for the repetitive firing phenomenon encountered in excitable membranes. Elegant papers by Arvanitaki (1939), Cole & Curtis (1941), Brink, Bronk & Larrabee (1941), pursued the subject, both experimentally and theoretically. Arvanitaki utilized for the first time the mathematics of Laplace to describe the limit cycles and trajectories involved in the excitation resulting in subthreshold oscillations and repetitive firing. Maintained oscillation and stability properties were considered in an early paper by Cole, Antosiewicz & Rabinowitz (1955) (also see FitzHugh & Antosiewicz (1959)), where, for the first time, threshold phenomena were

0022-3751/80/1230-0966 $07.50

explored using a plot of membrane potential (V) against rate of change of membrane potential (dV/dt or $\dot{V}$) derived from calculations of the theoretical model of the squid giant axon (Hodgkin & Huxley, 1952). Cole suggested to us that a V, $\dot{V}$ representation of a real squid axon membrane be attempted experimentally and its limit cycle behaviour be investigated on-line.

Both experimental and computational investigations have been carried out in the past on the abolition of an individual action potential by depolarizing or hyperpolarizing short shocks. The phenomenon was demonstrated experimentally by Hodgkin, Huxley & Katz (1949), who applied an anodal shock during the rising or falling phase of the action potential. It was also demonstrated by Weidmann (1951) during the plateau of the action potential of the conducting tissue of the kid heart and in the falling phase of the action potential at the node of Ranvier by Tasaki (1956). Huxley (1959) computed action potentials on the basis of the Hodgkin–Huxley (HH) equations and showed the effect of anodal displacement during the falling phase of his computed spike.

Experimental abolition of a repetitive spike train by a brief perturbation has apparently not been reported previously; although we have been recently made aware of an unpublished observation of annihilation of pace-maker activity by a brief perturbation in cardiac sinus node of kitten (Jose Jalife, personal communication; see *Note added in proof*). A number of theoretical studies suggest the possibility and provide motivation for this investigation.

Cooley, Dodge & Cohen (1965), as well as others (see Rinzel (1979) for references), studied repetitive firing in the HH model for current steps of various intensities. It was found, for a range of just suprathreshold intensities, $I_\nu < I < I_1$, that the equations have a stable steady-state solution (or singular point) which corresponds to steady depolarization in addition to the stable limit cycle of repetitive firing; here, I_ν is the threshold for a current step to elicit an infinite train.

The singular point exists for each value I. It loses stability as I increases through the critical value I_1 and regains stability as I increases through I_2; the singular point is unstable for $I_1 < I < I_2$.

Each of these stable states has its own domain of attraction which includes every initial state whose trajectory ultimately approaches the stable state. Cooley *et al.* pointed out that for a membrane model with two variables (but not necessarily more than two) this situation (the coexistence of a stable singular point and a stable limit cycle) demands the existence of an unstable limit cycle which separates the domains of attraction of these two stable states in the phase plane. Because the HH model has a four dimensional phase space, these domains of attraction are separated by a surface rather than by a single curve; this separatrix surface presumably contains the unstable limit cycles recently computed by Rinzel & Miller (1980) (for a summary see Rinzel, 1979). This structure suggests that the system trajectory could be forced across the separatrix surface from one domain of attraction to the other by a brief perturbation. Indeed, Cooley *et al.* showed that the system could be shocked out of the steady state. They demonstrated how a brief depolarizing pulse (superimposed on the steady bias current) perturbs the system away from the stable singular point and then the solution trajectory temporarily executes sub-

threshold oscillations (perhaps approximating the unstable limit cycle) which either damp to the singular point, if the perturbing pulse is too weak, or grow to the stable limit cycle if the pulse is sufficiently strong. The experimental results of Gregory, Harvey & Proske (1977) on 'regularly firing' stretch receptors suggest an analogous interpretation. They found that a shock, in the form of an antidromic action potential, was sufficient to initiate repetitive firing in a silent stretch receptor biased by a test stretch. The computational analysis of Best (1979) shows that one can also shock the HH system out of the repetitive mode. That is, with a properly timed and sized instantaneous current pulse one can force the system off the stable limit cycle and into the domain of attraction of the stable singular point. Annihilation of repetitive activity shocks was also demonstrated theoretically by Teorell (1971) for a two variable model.

The coexistence of two stable states in this way also implies that a system should exhibit hysteresis. Slow variations in current intensity back and forth across the entire range of values for which there is such coexistence would carry the system along in one state for a while and then cause the system to jump abruptly into and then back through the other state. A nerve with such characteristics would exhibit a sharp threshold of minimum current intensity for repetitive firing and a non-zero critical firing frequency at that level. It would also have a different critical current intensity for the onset of repetitive firing during a slowly rising ramp of current; it would not accommodate. The squid axon in low Ca has these features: see E. Jakobsson and R. Guttman (in preparation) for recent results on non-accommodation. In this study we demonstrate experimentally that these two critical current levels (analogous to I_v and I_1 in the HH model) are different.

In addition to these features associated with hysteresis, it was our goal to illustrate certain phase resetting behaviour which follows a brief current pulse delivered to the repetitively firing squid axon. Phase resetting characteristics have been classified and extensively discussed for biological oscillators, including neuronal examples, by Winfree (1977). Resetting data have been computed for the HH equations by Best (1979). Other neuronal examples may be found in Pavlidis & Pinsker (1977).

METHODS

Experimental

A freshly dissected squid giant axon was mounted in a chamber so that two flowing sucrose streams (0·8 M) isolated a central experimental region of the axon bathed in flowing low Ca artificial seawater solution (Fig. 1*A*). The two ends of the fibre were bathed by 0·5 M-KCl to inactivate those regions. The axon was stimulated with a current step by means of platinized Pt electrodes situated in one end compartment and in the flowing low Ca seawater central experimental region. The voltage response was monitored by means of two Ag–AgCl electrodes located in (1) the central experimental portion and (2) the other extreme compartment in KCl. Vaseline seals isolated the KCl compartments from the flowing sucrose. The central experimental portion was about 0·01 cm^2 in area.

Except on rare occasions, squid axons in seawater do not exhibit maintained repetitive firing under steady current clamp. However, they will fire repetitively with an infinite train in response to an adequate current step while bathed in low Ca seawater. If Ca concentration is too low then spontaneous oscillations may arise (Arvanitaki, 1939); this did not occur for the Ca concentration and experiments reported here.

The low Ca artificial seawater was made up as follows: NaCl, 545 mM; $CaCl_2$, 10 mM; KCl,

10 mM; Tris, 5 mM per litre in accordance with the general method of Frankenhaeuser & Hodgkin (1957) and pH was adjusted to 7·8. Normally there is about 35 mM-$CaCl_2$ in Woods Hole seawater. Experiments were done at temperatures near 22 °C and measured with a thermistor in artificial seawater near the axon. Actual temperatures are given in the Figure legends.

The experimental procedure was as follows. After the resting potential of the axon, whose central compartment was bathed in low Ca artificial seawater, had reached a steady state, threshold for repetitive firing was established by manually triggered stimulation with a step

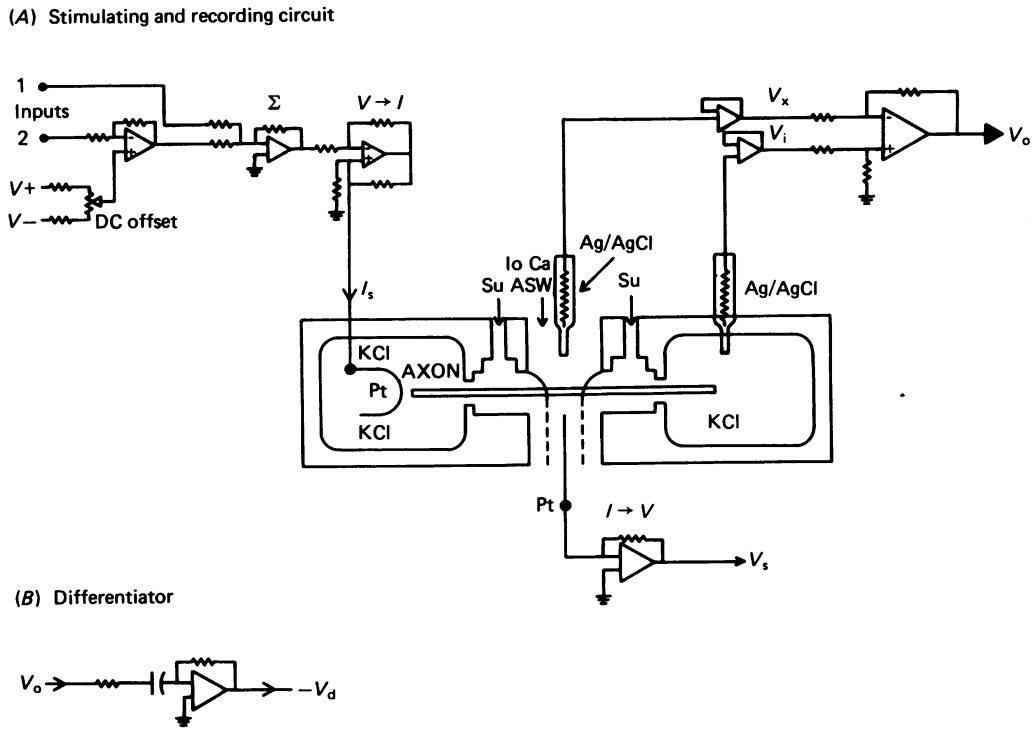

Fig. 1. *A*, instrumentation for study of repetitive firing in space-clamped squid axon. *B*, additional circuitry for displaying $\dot{V}$ *vs.* V trajectories.

of current, 30 msec in duration, to avoid overstimulation of the axon. Thereafter a slightly suprathreshold current step of approximately 30 msec duration was used as a bias in order to initiate repetitive firing. Upon this bias current, various magnitudes of brief 0·15 msec perturbations were added at various phases in the period of the response to investigate control of repetitive firing.

Current stimulation was applied to the axon via a Howland pump circuit (cf. V–I, Fig. 1*A*) which was driven by an amplifier that summed the desired inputs. I_s, the stimulating current, was fed through the axon and sensed by a virtual ground transresistance amplifier producing $V_s = 10^6 - I_s$. V_s was monitored on one channel of a Tektronix 564B storage oscilloscope.

The voltage response of the axon was monitored with Ag–AgCl electrodes connected to voltage followers. The outputs of the followers were connected to a difference amplifier to produce $V_0 = 100\ V_i - V_x)$, where V_i = inner potential, and V_x = external potential. V_0 was monitored on the other channel of the oscilloscope.

For experiments involving the trajectories of V *vs.* $\dot{V}(\dot{V} = \mathrm{d}V/\mathrm{d}t)$, $\dot{V}_0$ was fed into a differentiator to produce $V_d = -15 \times 10^{-6}\dot{V}_0$ (see Fig. 1*B*). The voltages V_s, V_o, and V_d were recorded simultaneously on an HP-3960 Instrumentation tape-recorder at 15 impulses/sec. Later the recorded information was played back at 15–16 impulses/sec to slow the trajectories

enough to enable the storage scope to write and to allow the data to be examined at various amplifications for detailed analysis.

Computational

Limit cycle solutions to the HH equations were computed directly by a finite difference method as outlined in Rinzel (1979) and described in more detail in Rinzel & Miller (1980). This technique differs from a forward-in-time integration of the equations and determines simultaneously the solution values at every point of a discrete mesh over the period of the limit cycle. The method is not sensitive to the stability of the periodic solution and was applied successfully for both stable and unstable limit cycles. These calculations were performed in double precision on the NIH/DCRT, IBM 370/168 digital computer system.

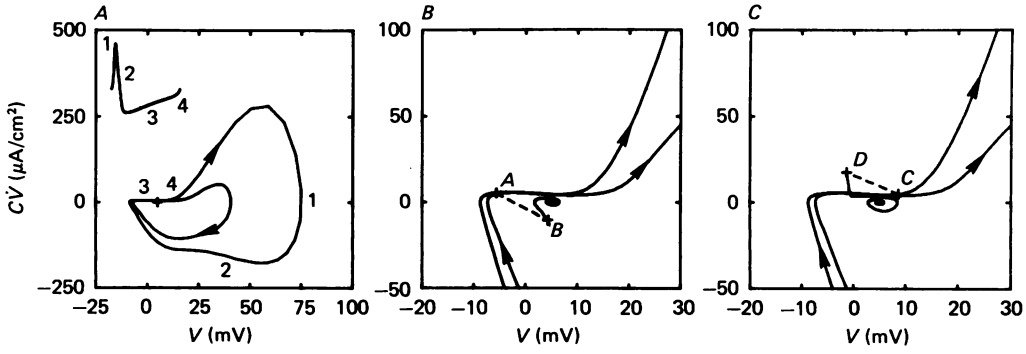

Fig. 2. *A*, simplified diagram to illustrate annihilation of repetitive firing for a current shock. Curves are V, $\dot{V}$ trajectories for computed solutions to HH equations, steady bias current 8·5 μA/cm². Temp. 18·5 °C. Outer (inner) closed curve is stable (unstable) limit cycle; singular, point shown with +. Inset shows V *vs.* t for stable limit cycle. *B*, depolarizing shock of 10 mV, delivered during period 3 causes instantaneous displacement ($A \rightarrow B$) off stable limit cycle and then annihilation. *C*, annihilation caused by hyperpolarizing shock of −10 mV delivered during period 4. Here displacement ($C \rightarrow D$) is to outside of V, $\dot{V}$ trajectory for stable limit cycle.

The transient trajectories for Figs. 2 and 10 were computed using the differential equation solver in the mathematical modeling program MLAB (Knott & Shrager, 1972) on the NIH/DCRT PDP-10 digital computer. The graphics capabilities of MLAB were used to produce Figs. 2, 9, 10, 11.

All theoretical calculations (illustrated in Figs. 2, 9, 10, 11) are for the standard HH equations with temperature of 18·5 °C. The model was used without the modifications of Huxley (1959) for the effects of low Ca. In order to illustrate and compare (experimental with theoretical) features which we view as qualitative, such as multiple stable states, annihilation and hysteresis phenomena, we consider the unmodified HH model as adequate.

RESULTS

Annihilation of repetitive firing

The following simplified diagram (Fig. 2) is offered in the hope of clarifying, for the reader, our results and interpretation. It is simplified in that we present trajectories in only the two dimensions V and $\dot{V}(\dot{V} = \mathrm{d}V/\mathrm{d}t)$ when a complete description of the system state would require many dimensions. In some experiments, these two variables were measured and used to display $\dot{V}$ *vs.* V trajectories (e.g. Fig. 7*B*).

Similar experimental trajectories for muscle were illustrated by Jenerick (1963). The trajectories in Fig. 2 were obtained numerically for the HH equations. In Fig. 2*A* the outer closed curve is the V, $\dot{V}$ trajectory of the stable limit cycle while the inner curve is the V, $\dot{V}$ trajectory for the unstable limit cycle. Here the bias current is 8·5 μA/cm^2 and temperature is 18·5 °C. The stable singular point in these coordinates is shown with $a+$ on the axis $\dot{V} = 0$. Different phases of the stable cycle are numbered to correspond to the V *vs.* t profile (action potential) shown in the inset.

Intuitively, one might picture the stable limit cycle as a valley and the separatrix surface, wherein lies the unstable limit cycle, as being at the top of a hill. Then any perturbation sufficient to propel the trajectory over that hill will cause it to drop into a hole represented by the stable singular point which is surrounded by the separatrix surface. Annihilation of repetitive firing then results. For the HH model, an instantaneous current pulse or shock at $t = t_0$ causes a jump in V, and also in $\dot{V}$, proportional to pulse strength (this is explained with more detail in the discussion section). Hence, for such a perturbation, the state point is instantaneously displaced off the stable limit cycle and also off its V, $\dot{V}$ trajectory. In Fig. 2*B*, on an enlarged scale, the crosses and dashed line segment $A \rightarrow B$ represent the displacement for a depolarizing shock of 10 mV. This shows the subsequent annihilation with damping to the singular point.

We remind the reader however that this two dimensional representation has its limitations. Just as the shadow of a three dimensional object does not reveal its surface dimples and bumps so a two dimensional projection does not adequately reveal the structure of the four dimensional phase space: the separatrix surface, the trajectories and limit cycles. The V, $\dot{V}$ trajectories may cross one another or even themselves while this is ruled out for the actual four dimensional trajectories. Furthermore, even though a shock may displace the V, $\dot{V}$ point for the system state vector to the inside of the V, $\dot{V}$ unstable limit cycle this does not imply necessarily that the actual state vector in four dimensions has crossed the separatrix surface into the domain of attraction of the singular point. Conversely, a shock could displace the state vector across the separatrix surface but the V, $\dot{V}$ representation may not reveal this. Fig. 2*C* offers such an example. Here the parameters are the same as previously except a hyperpolarizing shock (-10 mV) is presented at a later phase. The displacement $C \rightarrow D$ leaves the V, $\dot{V}$ point outside the V, $\dot{V}$ represented stable limit cycle. The resultant V, $\dot{V}$ trajectory crosses both limit cycle representations as annihilation ensues.

The experimental results (Figs. 3–8) will now be presented along with some interpretation motivated by the above theoretical considerations.

The central experimental portion of a freshly dissected space-clamped squid axon was bathed in low-Ca solution and when the monitored resting potential reached a steady state, it was then stimulated with a barely suprathreshold step of current, of 30 msec duration, which caused it to enter the repetitively firing condition (Fig. 3*A*, upper half; stimulus (above) and response (below)). Then at a subsequent 30 msec duration suprathreshold stimulus, while the axon was in the repetitively firing mode, a brief depolarizing pulse (or hyperpolarizing one in the case of Fig. 7) of 0·15 msec duration was superimposed upon the step of suprathreshold current. In the case of Fig. 3*A*, lower half, this depolarizing perturbation was sufficient in magnitude and delivered at just the proper phase to completely annihilate the repetitive firing. Notice that the trace thereafter is quite flat. This indicates that in this particular case the perturbation probably forced the system trajectory across the separatrix

surface and so near to the singular point, that the trajectory entered the singular point directly without noticeably spiralling into it.

Theoretically, if a second pulse of adequate size is applied following annihilation the trajectory will be sent back out across the separatrix surface and return to the limit cycle. An experimental demonstration of this would show also that the first pulse did not destroy the membrane's *capability* to fire repetitively for this bias current. Although we did not carry out this direct test, the fact that successive runs still showed reliable repetitive firing for the bias step provides sufficient evidence.

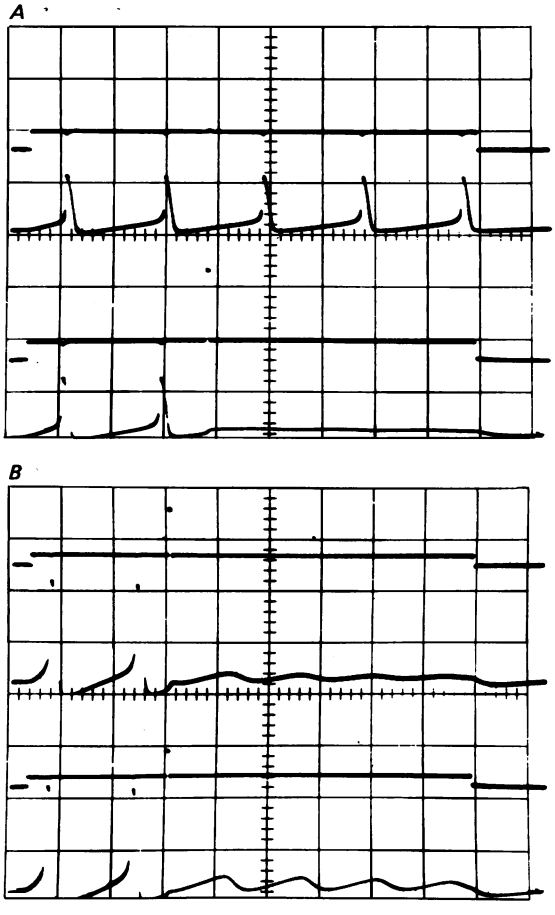

Fig. 3. *A*, annihilation of repetitive firing of space-clamped squid axon membrane by a brief depolarizing perturbation. Calibration: 100 mV/div, 2 μA/div, 2 msec/div. Temp. 22·3 °C. *B*, annihilation of repetitive firing for two different brief depolarizing pulses. Note that degree of damping of subthreshold oscillations (trajectories) depends on magnitude of shock. Calibration: 50 mV/div; 5 μA/div; 2 msec/div. Temp. 22 °C.

In Fig. 3*B* upper and lower halves, the trajectory resulting from the perturbation does not enter the singular point so directly. The trajectory evidently spirals inward before dropping into the singular point and this is evidenced in the form of subthreshold oscillations. In the upper half of Fig. 3*B*, where the magnitude of the perturbing pulse is greater, the damping of the subthreshold oscillations is more

marked than in the lower half, where the perturbation is of lesser magnitude. In the latter case the perturbation evidently left the trajectory farther from the singular point and closer to the separatrix surface. Theoretically, in a noiseless system, a direct hit onto this surface would find the trajectory forever restricted to it; it is an invariant surface in the phase space.

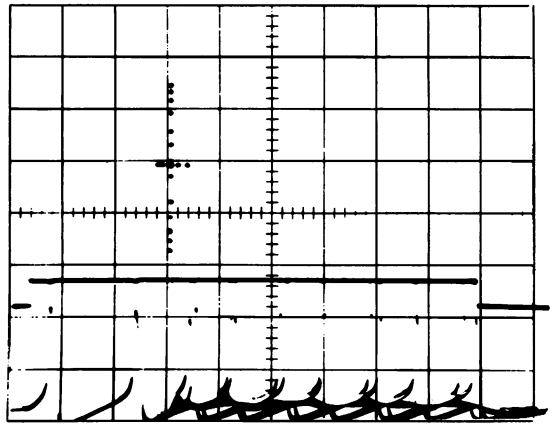

Fig. 4. Mapping of experimental parameter values for annihilation of repetitive firing. Calibration: 50 mV/div; 2 μA/div; 2 ms/div. Temp. 22·4 °C.

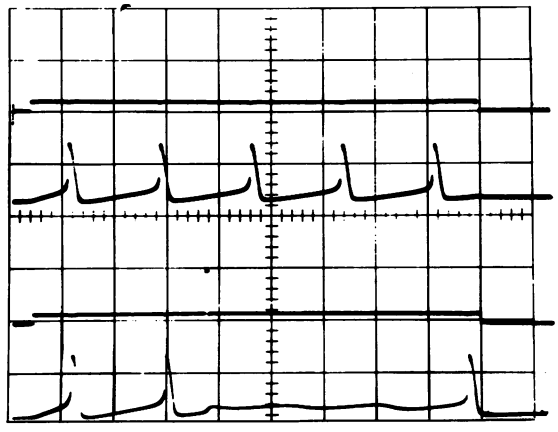

Fig. 5. Perturbation of a repetitively firing axon membrane by a brief depolarizing shock which does not cause annihilation. Note ultimate return to stable limit cycle (spike) with phase resetting. Calibration: 100 mV/div; 5 μA/div, 2 ms/div. Temp. 22·4 °C.

Fig. 4 represents one of a number of attempts to plot roughly the region in pulse parameter space for annihilation by varying the magnitude and phase of the perturbing pulse. Such regions are referred to as access portals by Best (1979) or described as vulnerable regions by Teorell (1971). The perturbations which vary in magnitude (represented by dots forming the vertical bar of the cross) and phase (represented by dots forming the horizontal bar of the cross) all resulted in annihila-

tion of repetitive firing except for the four extreme dots. These four exceptions resulted in phase resetting. The region for annihilation corresponds to perturbations of a few mV up to 15–20 mV delivered somewhat following the peak after-hyperpolarization phase of the spike, period 3 of Fig. 2*A*. Thus, the region for annihilation can be mapped roughly. This was technically a difficult experiment to carry out. (It was necessary to watch the moving response trace to determine effectiveness or lack of effectiveness regarding annihilation.)

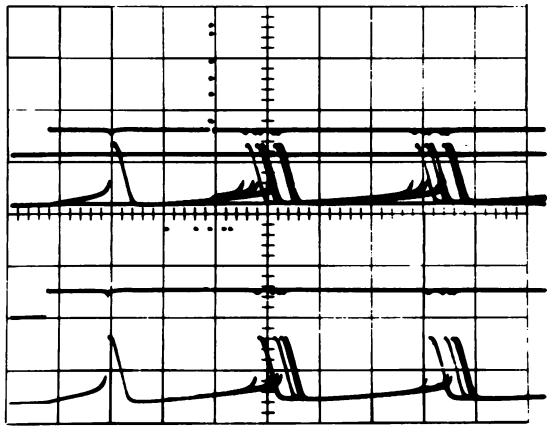

Fig. 6. Phase resetting by depolarizing perturbations of a repetitively firing axon membrane. Perturbations vary in magnitude (above) and in phase (below). Records superimposed on CRO. Calibration: 100 mV/div; 2 μA/div; 1 ms/div. Temp. 21·7 °C.

In Fig. 5, lower half, the brief pulse has presumably forced the trajectory near to, but not across, the separatrix surface. This is not a case of annihilation. The trajectory apparently spirals *outward* and reaches the stable limit cycle, causing the axon to return to the repetitively firing mode. The gain on the scope is higher than in Fig. 3*B*, but still one can see the subthreshold oscillations grow and then finally explode into a spike. The trajectory asymptotically enters the stable limit cycle at a point that results in phase resetting. While the frequency of the new repetitive firing proves to be identical with that of the old frequency, one can see that re-entry into the stable limit cycle occurred at a point such that the new phase is shifted compared to the extrapolated original train of spikes.

Phase-resetting

In Fig. 6, magnitude (above) and phase (below) of the perturbing pulse were again varied as in Fig. 4. But in this type of experiment the purpose was different. This figure represents a demonstration of the effect of magnitude and time delay of the depolarizing perturbation upon phase resetting. Unfortunately, the data were not obtained in such a way as to allow quantification of the resetting characteristics and precise comparison with theoretical predictions for the HH model. Nevertheless, the fact that resetting can be observed is consistent with the idea that the oscillation is indeed an autonomous limit cycle. The response record for the upper (lower) portion of Fig. 6 represents six (five) traces superimposed. For the range of pulse

phases in the lower portion we find that as the perturbation is applied later, the new spike is first pulled to the left and then recedes back to the right. This increasing, then decreasing, phase advance is in qualitative agreement with a set of HH calculations for pulses ($\Delta V = 4$ mV, bias of 20 μA/cm^2) applied through a range of phases in the action potential trough (period 3 of Fig. 2*A*).

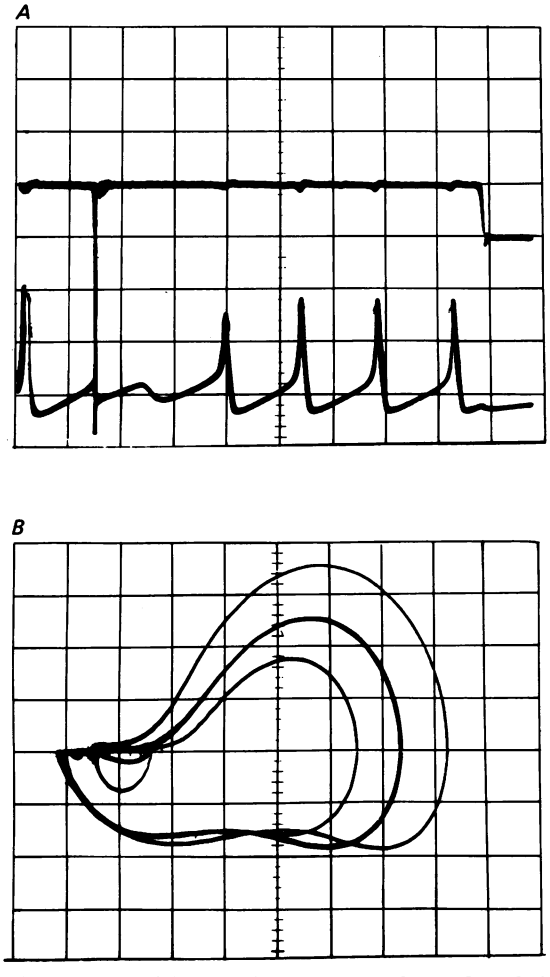

Fig. 7. *A*, perturbation of a repetitively firing axon membrane by a brief hyperpolarizing pulse delivered at the rising phase of a spike. Calibration: 50 mV/div; 2 μA/div; 2 msec/div. Temp. 24·7 °C. *B*, same response data displayed on storage CRO after voltage and $\dot{V}$ were recorded on two channels of a tape recorder and played back at diminished speed. Calibration: $\dot{V}$ (vertical) ~ 200 V/sec. div; horizontal ~ 20 mV/div. Temp. 24·7 °C.

Phase resetting was observed for hyperpolarizing pulses as well as depolarizing pulses. Annihilation of repetitive firing could also be achieved with appropriate hyperpolarizing pulses; examples were found for pulses delivered during the early rising phase, period 4 of Fig. 2*A*.

In Fig. 7*A*, current and voltage are traced *vs.* time on the oscilloscope face as in the

preceding figures, showing the current step with the hyperpolarizing shock delivered at the rising phase of what would have been a second spike in the response trace. While the perturbation is being delivered the rise of voltage is abruptly terminated

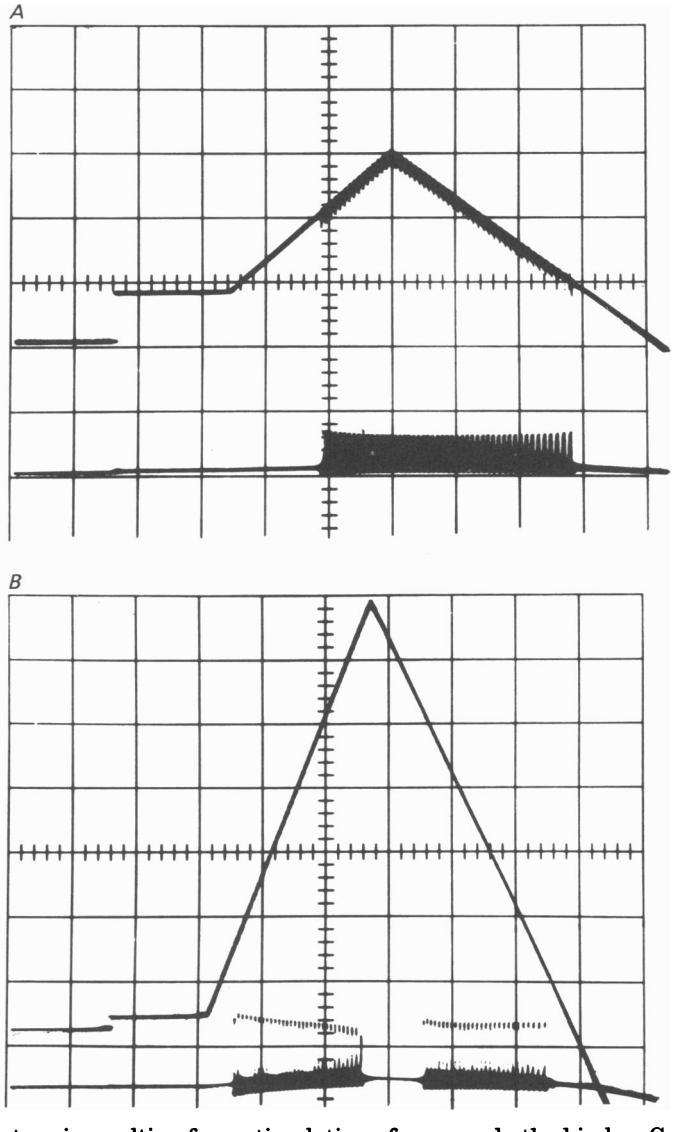

Fig. 8. *A*, hysteresis resulting from stimulation of an axon bathed in low Ca by a ramp current stimulus. Calibration: 100 mV/div; 1 μA/div; 50 msec/div. Temp. 22·0 °C. *B*, hysteresis and cut-off at high intensity of repetitive firing in an axon stimulated by ramp currents. Calibration: 50 mV/div; 2 μA/div; 50 msec/div. Temp. 20·2 °C.

with a considerable negative $\dot{V}$ component. The following subthreshold response is less steep in its rising and falling phases. These characteristics permit us to trace the clockwise trajectories in Fig. 7*B*, where $\dot{V}$ is now plotted *vs.* V by the axon in a record which has been slowed down (cf. Methods). The largest trace represents the

trajectory of the first (largest) spike in Fig. 7*A*. The innermost loop traces the trajectory of the subthreshold oscillation, where $\dot{V}$ is least negative. The slightly larger U loop represents the trajectory during the perturbation, where $\dot{V}$ is somewhat more negative. The smallest spike is represented by the smallest of the three large trajectories. The final spikes, which are intermediate in size, are represented by three superimposed traces: the middle of the three large trajectories.

Ramp stimulation and hysteresis

Finally, to directly demonstrate hysteresis, slowly rising and falling current ramps were used to observe the nerve switch from the steady state to the repetitive firing mode and vice versa. For hysteresis, these switch points differ during the rising and falling of the stimulus. As before, the axon was bathed in low Ca. It was stimulated by a step of current upon which a linearly rising or falling ramp of current was superimposed. It is very clear (Fig. 8*A*) that the onset of firing occurs at a higher stimulus current intensity than the cessation of repetitive firing.

In Fig. 8*B*, the rising current was allowed to reach much higher than in Fig 8*A*. It rose so high that repetitive firing was cut off and the membrane returned to the depolarized and apparently restabilized steady state. The cut off is similar to impulse block seen with overstretch in some stretch receptors (Terzuolo & Washizu, 1962). In this record one observes four different switch points. The two on the up ramp are different from the two on the down ramp. Evidently there are hysteresis loops at both the lower intensity onset and the upper intensity cut off of repetitive firing.

DISCUSSION

This work shows that repetitive firing in a patch of squid axon membrane pursues a limit cycle oscillation. As an oscillator, the membrane exhibits phase resetting in response to brief perturbations. Moreover, near threshold it is a hard oscillator. That is, we find two critical values of current intensity for the onset of repetitive firing; a lower one for a suddenly applied stimulus (for example, a step perhaps with a superimposed initial perturbing pulse) and an upper one for a slowly increasing ramp. In the range between these two values, a stable steady-state coexists along with the stable limit cycle for repetitive firing. Consequently, hysteresis and switching are observed when current is slowly swept back and forth through this range. For a stimulus which approaches a steady level in this range, the adapted response depends on how that steady level is attained. Moreover brief perturbations of appropriate strength and phase, when superimposed on a bias current (tuned into the range for coexistence), will annihilate repetitive firing with the system exhibiting damped oscillations to the steady state. These experimental findings compare qualitatively to theoretical results for the standard HH equations.

While the experimental and theoretical results are in qualitative agreement in that they show hysteresis at the lower threshold, there is disagreement at the upper intensity cutoff. Fig. 8*B* shows an experimental example of hysteresis at the upper range. In contrast, the theoretical model does not exhibit hysteresis at this end. For the standard HH equations, the stable limit cycle disappears for large enough bias current but in this case it gradually shrinks to zero amplitude (with increasing bias) collapsing down onto the singular point as the latter regains its stability.

The theoretical results (Best (1979), Cooley *et al.* (1965), Rinzel & Miller (1980) and their references) provided substantial motivation for these experiments.

Annihilation, hysteresis, and some of their functional implications

We do not consider such features to be restricted only to the repertoire of squid nerve or of the HH model. One might reasonably expect to observe similar characteristics for some other neural elements and likewise some other mathematical models (even if they possess additional ionic currents such as in Connor & Stevens (1971)) which exhibit repetitive firing for a maintained stimulus. The observation of a sharp (minimum) threshold in steady stimulus intensity for repetitive firing with a non-zero firing frequency at that level, along with a lack of accommodation, strongly suggests the possibility of coexistence and hysteresis. We remark that the 'integrate and fire' model (e.g. see Knight (1972)) which has a minimum firing frequency of zero at threshold does not have coexistent stable states and cannot account for hysteresis and annihilation phenomena. In the case of hysteresis, the range of intensities for coexistence, called the overlap range by Rinzel (1979), $I_v < I < I_1$, will of course depend on environmental parameters (temperature, ionic composition of bath, etc.) and on membrane characteristics. For the standard HH model, the dependence of I_v and I_1 on temperature has been computed (Rinzel & Miller, 1980; Rinzel, 1979). The difference I_1–I_v decreases to zero as temperature approaches a critical value, 28·85 °C, above which there is no repetitive firing for any steady current. In Fig. 8*B* the overlap range is about 5 % of the total range for repetitive firing; at the higher intensity cut-off, the overlap is 25 % or more.

Even if the overlap is not large relative to the total range for repetitive firing, its existence has an obvious consequence for behaviour near threshold. Once the stimulus intensity is tuned into this overlap range, the adapted state, either steady or repetitive firing, is well determined and stable. Small perturbations will not cause switching. A nerve without overlap and when operating near threshold may be thrown into and out of the repetitive mode by very small fluctuations. Presumably then, coexistence with hysteresis enhances stability and increases efficiency near threshold. This was also pointed out for a model of activity in a neuronal population by Wilson & Cowan (1972). Switching behaviour in a variety of physical systems (e.g. heating thermostats) are designed this way to prevent inefficiency from excessive on-off switching.

In the overlap range, the relative size of the domain of attraction and strength of attraction for each of the two stable states depends on the value to which the intensity is set in the overlap range. Let us first interpret this in terms of the HH model. For $I < I_v$, there are no limit cycle solutions and the singular point is the only attractor. The entire phase space is its domain of attraction, i.e. it is globally attracting. As I is increased with $I_v < I < I_1$ the domain of attraction of the singular point becomes smaller and shrinks to zero as I tends to I_1. For a range of $I > I_1$, the singular point is unstable and only the stable limit cycle has a nontrivial domain of attraction. To describe the domains of attraction by numerical estimation of the separatrix surface would require considerable effort. As an alternative we consider Fig. 9 which gives some indication of the relative sizes for I in the overlap range. It shows the stable and unstable limit cycles (outer and inner curves) projected to the V, n plane (here, n

is the HH variable, K activation) for four values of I satisfying $I_v < I < I_1$ where $I_v = 8{\cdot}031\ \mu A/cm^2$, $I_1 = 18{\cdot}564\ \mu A/cm^2$ and temperature is 18·5 °C. In the upper left frame where $I = 8{\cdot}05\ \mu A/cm^2$, the two limit cycles are very close together. They arose as a pair from the splitting of a neutrally stable limit cycle which exists, as a single one, only for $I = I_v$. As I increases, the unstable limit cycle gets smaller and

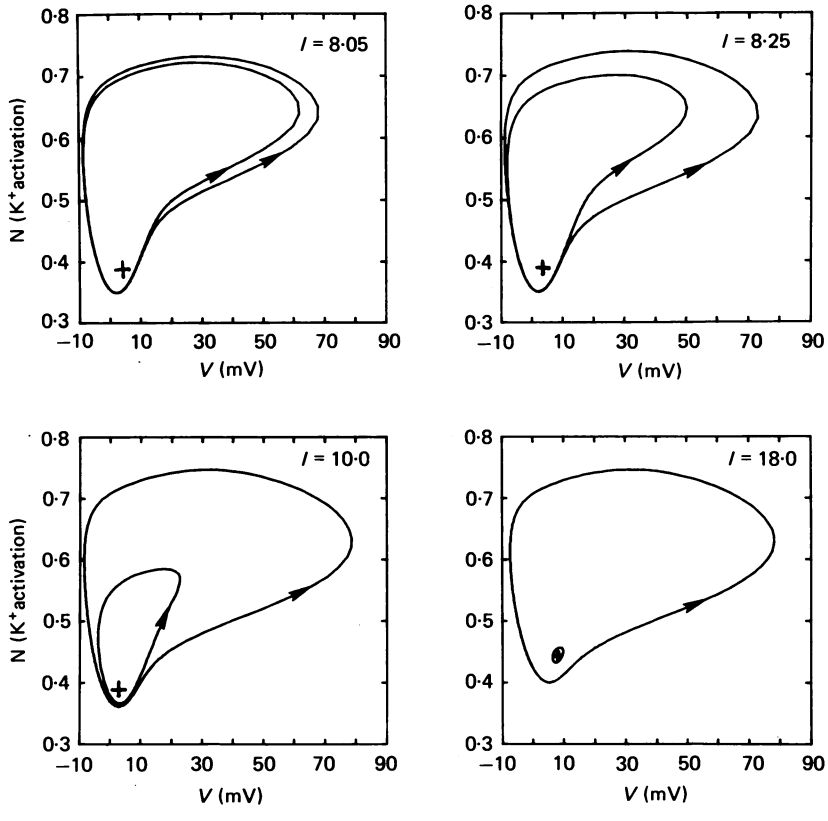

Fig. 9. Projections, n *vs.* V, of stable (outer curve) and unstable (inner curve) limit cycle solutions to HH equations for four values of steady current I ($\mu A/cm^2$). Temp. 18·5 °C. Singular point, shown with $a+$, is stable for these values of I.

shrinks onto the singular point as I tends to I_1. This description, qualitatively correlates with our experimental findings as follows. In some axons the range of pulse strengths and phases for annihilation was so small that attempts to map it had to be abandoned. Moreover it was also noticed that in a given axon preparation if the bias step was maintained barely over threshold, the range of pulse parameters for annihilation proved to be larger.

In this paper we have illustrated and discussed coexistence and hysteresis phenomena with respect to an applied current. One should keep in mind that such behaviour could be exhibited with respect to other parameters as well. For example, with adjustments in the HH model for altered external Ca concentration, Huxley (1959) estimated the overlap range with respect to Ca concentration for a fixed bias intensity.

As a further example, consider the 'skip runs' (spikes with intervening small subthreshold oscillations in definite patterns) found experimentally in the real squid axon (Guttman & Barnhill (1970)). They may be due to an oscillating parameter with a period of about 15 msec at 25 °C and 20 msec at 15 °C. During the increasing phase of the parameter the membrane would be operating in one mode, either the repetitive firing mode or else near the steady-state mode as evidenced by the small subthreshold oscillations. During the parameter's decreasing phase it would be in the other mode. The physiological parameter could conceivably be coupled intrinsically to the system but on a slower time scale.

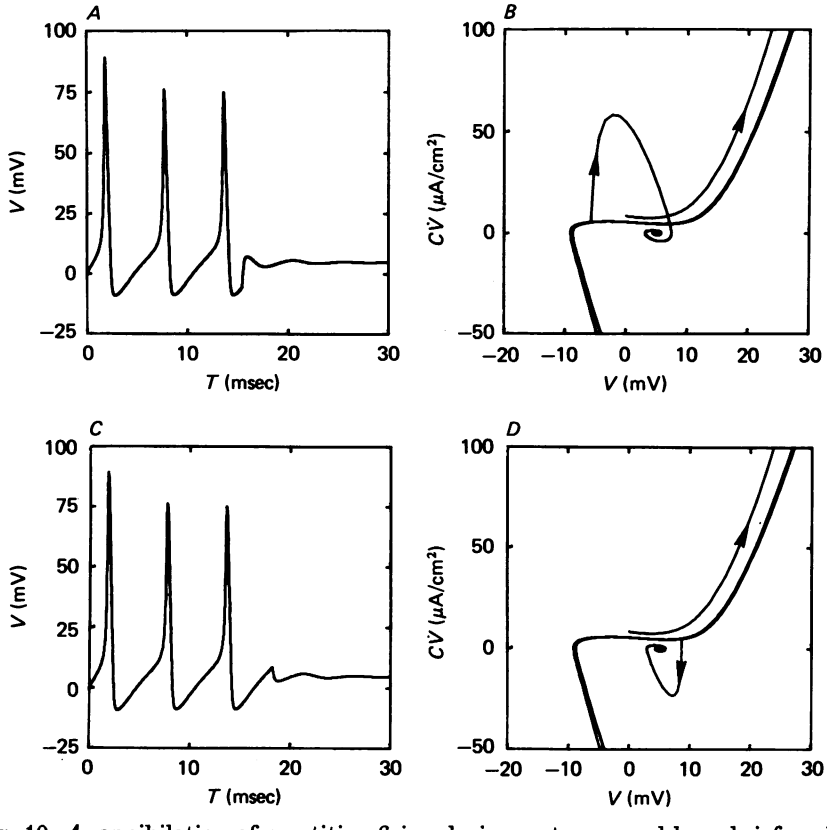

Fig. 10. *A*, annihilation of repetitive firing during a step caused by a brief excitatory synaptic input. *V vs. t*, computed from HH equations. Synaptic current and conductance given by (1) and (2). Bias intensity 8·5 μA/cm². Temp. 18·5 °C. *B*, *V*, $\dot{V}$ trajectory corresponding to solution described in *A*. Expanded scale here shows annihilation with damped oscillations to singular point. *C*, *D*, same as *A* and *B*, except here annihilation of repetitive firing during a step is caused by a brief inhibitory synaptic input.

Stabilization against noise is one functional consequence of hysteresis. An additional functional interpretation is suggested when one considers that a neuronal oscillator with a coexistent steady state can be turned on or off by a brief stimulus. This possibility could be exploited for a neurone being used as a time keeper or pacemaker for some finite duration or as a source to provide a long train of spikes

until signalled to stop. In such cases the membrane might naturally be biased to the overlap range and normally silent. The repetitive mode could be initiated and terminated by a brief stimulus e.g. transient synaptic input. Because an exogenous source, e.g. continued synaptic bombardment, would not be required to maintain repetitive firing, this might be considered an efficient way to utilize the oscillator. Moreover the on-off switching could be accomplished by either excitatory or inhibitory inputs of appropriate timing and size.

To illustrate this we have computed solutions to the HH equations for which a brief synaptic event is superimposed on a current step; the step intensity, 8·5 μA/cm^2, is tuned to the overlap range. The synaptic current is represented as a transient conductance change which multiplies a driving potential:

$$I_{\text{syn}}(t) = G_{\text{syn}}(t)(V - \bar{V}_{\text{syn}}), \tag{1}$$

where

$$\left.\begin{aligned} G_{\text{syn}}(t) &= \bar{G}_{\text{syn}}\,\tau_{\text{syn}}^{-1}(t-t_0)\exp\left[1-\tau_{\text{syn}}^{-1}(t-t_0)\right] \quad \text{for} \quad t \geqslant t_0 \\ &= 0 \qquad\qquad\qquad\qquad\qquad\qquad\qquad\quad \text{for} \quad t < t_0 \end{aligned}\right\} \tag{2}$$

This form for $\bar{G}_{\text{syn}}(t)$ was used by Rall (1967). It begins its rise from zero at $t = t_0$, takes a peak value of $\bar{G}_{\text{syn}}$ at $t = t_0 + \tau_{\text{syn}}$ and then tends to zero asymtotically for large t. Fig. 10A and 10B show how the oscillator may be turned off by an excitatory input for which $\tau_{\text{syn}} = 0{\cdot}1$ msec, $\bar{G}_{\text{syn}} = 0{\cdot}5$ mmho/cm^2 and $\bar{V}_{\text{syn}}$ is set to the Na equilibrium potential $\bar{V}_{\text{Na}}$. Fig. 10A illustrates V *vs.* t while Fig. 10B gives the V, $\dot{V}$ trajectory on an expanded scale (as in Fig. 2B and C). In this latter plot, one may identify the first spike as initiating from $V = 0, C\dot{V} = 8{\cdot}5\ \mu$A/cm^2 and the two successive ones nearly superimposed as they approach the stable limit cycle. The inverted U loop corresponds to the depolarizing current during the synaptic event and the subsequent annihilation is evidenced by the trajectory spiraling into the singular point. For Fig. 10C and D, the synaptic input is inhibitory ($\bar{G}_{\text{syn}} = 1{\cdot}5$ mmho/cm^2, $\tau_{\text{syn}} = 0{\cdot}1$ msec, $\bar{V}_{\text{syn}} = V_{\text{K}}$) but delivered at a phase different from that in Fig. 10A and B. In this case also, annihilation of repetitive firing is observed. In these examples, the perturbing current is smooth and results in smooth V, $\dot{V}$ trajectories as compared to the jumps illustrated in Fig. 2B and C.

V, $\dot{V}$ Displacement for current pulse

If the perturbing pulse is brief enough, then it may be represented mathematically as a shock, i.e. a charge Q instantaneously placed across the membrane capacity. Suppose this occurs at $t = t_0$, then the change in voltage caused by this pulse of displacement current is

$$\Delta V = V(t_0^+) - V(t_0^-) = Q/C \tag{3}$$

where C is the membrane capacity. For any HH-like model the membrane conductances do not change instantaneously however the ionic currents do because of the jump in V. To see this we write $I_{\text{ion}}(t, V)$ as the sum

$$I_{\text{ion}}(t, V) = \sum_j G_j(t)\,(V - \bar{V}_j)$$

where $G_j(t)$ is the membrane conductance for ion species 'j' and $\bar{V}_j$ is the associated

equilibrium potential. Then, using continuity of G_j at $t = t_0$, the jump in ionic current is

$$\begin{aligned}\Delta I_{\text{ion}} &= I_{\text{ion}}(t_0^+) - I_{\text{ion}}(t_0^-) \\ &= \Sigma G_j(t_0)\,[V(t_0^+) - V(t_0^-)] \\ &= \Delta V \sum_j G_j(t_0) \\ &= \Delta V G_m(t_0), \end{aligned} \tag{4}$$

where $G_m(t_0)$ is the total membrane conductance or chord conductance at $t = t_0$. Current balance for the membrane requires

$$C\dot{V} = -I_{\text{ion}} + I_{\text{app}}(t), \tag{5}$$

where I_{app} is the applied current bias. From (4) and (5) it follows that

$$\Delta\dot{V} = -\Delta V G_m(t_0)/C. \tag{6}$$

Thus (3) and (6) give the displacement of V and $\dot{V}$ for an instantaneous current pulse. Examples are illustrated in Fig. 2*B* and *C* for the HH model. We further see from (6), since $G_m > 0$, that ΔV and $\Delta\dot{V}$ have opposite sign. In particular, as seen in Fig. 2*C*, a hyperpolarizing pulse during period 4 (before $\dot{V}$ reaches its maximum) must displace the V, $\dot{V}$ trajectory to the outside of the V, $\dot{V}$ representation of the stable limit cycle. In the case of subsequent annihilation, this observation a priori predicts that V, $\dot{V}$ trajectories must cross.

The derivation above further suggests a procedure for measuring G_m at any phase during the limit cycle. From (6), the slope $\Delta\dot{V}/\Delta V$ of the instantaneous displacement vector for the V, $\dot{V}$ trajectory, in response to a current shock, is equal to $-G_m/C$. To demonstrate, we have computed $\Delta\dot{V}$ for a shock of $\Delta V = -5$ mV at eight different phases of the stable limit cycle for the HH equations. The displacements are shown in Fig. 11. The crosses on the V, $\dot{V}$ trajectory of the limit cycle correspond to t_0^- and the remaining crosses correspond to the displacement at t_0^+. Line segments connecting the crosses are shown for ease of identification and comparison; they do not represent part of the solution trajectory. The subsequent trajectory after each current shock is not shown. The conductance increases during the upstroke (period 4 of Fig. 2*A*), reaches a maximum near the action potential peak, decreases but remains fairly large during the falling phase, and is small during the action potential trough (period 3). Cole (1968, fig. 3:53) has analogously illustrated membrane conductance on a two variable plot of the membrane current versus voltage trajectory for a propagated HH action potential; without space-clamp control however, a simple measurement procedure for G_m from the effect of a perturbing pulse does not present itself.

Although the pulse we applied experimentally was brief (0·15 msec) it was not an instantaneous shock. For this, the pulse duration should be short relative to the time scale of Na activation at the operating temperature. Unfortunately, in our recordings the V, $\dot{V}$ response during the current pulse appears rounded rather than square (cf. Fig. 7*B*). It would be difficult to estimate the displacement caused by the current pulse. The roundedness may be due to band-limited characteristics of our tape re-

corder or some other reason. Nevertheless, this method for measuring G_m should work in principle. Moreover, it could be implemented along with a phase-resetting study.

In conclusion, the membrane exhibits a hard oscillation with two stable modes of behaviour, one large amplitude and oscillatory and the other a time independent steady-state. A surface in the phase space separates the two attractor basins; trajectories tend to travel away from the surface toward either of the two attractors.

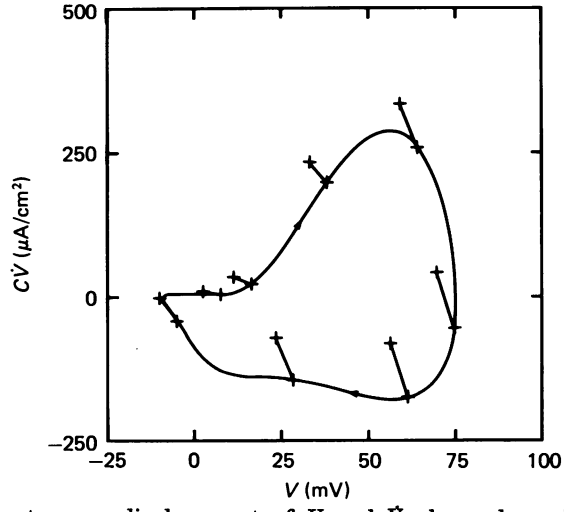

Fig. 11. Instantaneous displacement of V and $\dot{V}$, shown by +'s, for current shock of -5 mV at different phases of HH stable limit cycle. Total membrane conductance G_m is proportional to slope of displacement vector, $-G_m/C$.

Perhaps, as also suggested by Teorell (1971), these concepts might be more commonly introduced in excitation physiology to provide a better formal understanding of repetitive firing, threshold for repetitive firing, and excitation and inhibition phenomena.

Note added in proof. Subsequent to acceptance of this manuscript we learned of a much earlier observation by Chapman (personal communication) of annihilation by a brief depolarizing pulse of repetitive firing in the giant axon of squid (*Loligo vulgaris*). Also, subsequent to acceptance of this manuscript, observations of phase-resetting and annihilation of cardiac pace-maker activity have been reported by J. Jalife & C. Antzelevitch (1979): Phase resetting and annihilation of pacemaker activity in cardiac tissue. *Science, N.Y.* **206**, 695–697.

We have discussed this work with many and wish to acknowledge their help, especially Drs K. S. Cole, H. Fishman, W. Rall, and F. A. Dodge.

This work was aided in part by N.I.H. grant 5 RO1 NS 12272 awarded to R. Guttman. Apparatus loaned by Dr Fishman was purchased under his grant, N.I.H. NS 11764.

REFERENCES

ARVANITAKI, A. (1939). Recherches sur la réponse oscillatoire locale de l'axone géant isole' de 'Sepia'. *Archs int. Physiol.* **49**, 209–256.

BEST, E. N. (1979). Null space in the Hodgkin–Huxley equations. A critical test. *Biophys. J.* **27**, 87–104.

BRINK, F., BRONK, D. W. & LARRABEE, M. G. (1941). Chemical excitation of nerve. *Ann. N.Y. Acad. Sci.* **47**, 457–485.

COLE, K. S., ANTOSIEWICZ, H. A. & RABINOWITZ, P. (1955). Automatic computation of nerve excitation. *J. Soc. indust. appl. Math.* **3**, 153–172.

COLE, K. S. (1968). *Membranes Ions and Impulses*, p. 314. Berkeley: University of California Press.

COLE, K. S. & BAKER, R. F. (1941). Transverse impedance of the squid giant axon during current flow. *J. gen. Physiol.* **24**, 535–549.

COLE, K. S. & CURTIS, H. J. (1941). Membrane potential of the squid giant axon during current flow. *J. gen. Physiol.* **24**, 551–563.

CONNOR, J. A. & STEVENS, C. F. (1971). Prediction of repetitive firing behaviour from voltage clamp data on an isolated neurone soma. *J. Physiol.* **213**, 31–53.

COOLEY, J., DODGE, F. & COHEN, H. (1965). Digital computer solutions for excitable membrane models. *J. cell. comp. Physiol.* **66**, 99–108.

FITZHUGH, R. & ANTOSIEWICZ, H. A. (1959). Automatic computation of nerve excitation-detailed corrections and additions. *J. Soc. indust. appl. Math.* **7**, 447–458.

FRANKENHAEUSER, B. & HODGKIN, A. L. (1957). The action of calcium on the electrical properties of squid axon. *J. Physiol.* **137**, 218–244.

GREGORY, J. E., HARVEY, R. J. & PROSKE, U. (1977). A late supernormal period in the recovery of excitability following an action potential in muscle spindle and tendon organ receptors and its effect on their responses near threshold for stretch. *J. Physiol.* **271**, 449–472.

GUTTMAN, R. & BARNHILL, R. (1970). Oscillation and repetitive firing in squid axons. *J. gen. Physiol.* **55**, 104–118.

HODGKIN, A. L. & HUXLEY, A. F. (1952). A quantitative description of membrane current and its application to conduction and excitation in nerve. *J. Physiol.* 500–544.

HODGKIN, A. L., HUXLEY, A. F. & KATZ, B. (1949). Ionic currents underlying activity in the giant axon of the squid. *Archs Sci. physiol.* **3**, 129–150.

HUXLEY, A. F. (1959). Ion movements during nerve activity. *Ann. N.Y. Acad. Sci.* **81**, 221–246.

JENERICK, H. (1963). Phase plane trajectories of the muscle spike potential. *Biophys. J.* **3**, 363–377.

KNIGHT, B. W. (1972). Dynamics of encoding in a population of neurons. *J. gen. Physiol.* **59** 734–766.

KNOTT, G. D. & SHRAGER, R. (1972). *On-line Modeling by Curve-Fitting.* Computer Graphics: Proceedings of the SIGGRAPH Computers in Medicine Symposium. ACM SIGGRAPH Notices, vol. 6, no. 4, pp. 138–151.

PAVLIDIS, T. & PINSKER, H. M., eds. (1977). Workshop proceedings Oscillator Theory and Neurophysiology. *Fedn Proc.* **36**, 2033–2059.

RALL, W. (1967). Distinguishing theoretical synaptic potentials computed for different soma-dendritic distributions of synaptic input. *J. Neurophysiol.* **30**, 1138–1168.

RINZEL, J. (1979). On repetitve activity in nerve. *Fedn Proc.* **37**, 2793–2802.

RINZEL, J. & MILLER, R. N. (1980). Numerical calculation of stable and unstable periodic solutions to the Hodgkin–Huxley equations. *Math. Biosci.* (in the Press).

TASAKI, I. (1956). Initiation and abolition of the action potential of a single node of Ranvier. *J. gen Physiol.* **39**. 377–395.

TEORELL, T. (1971). A biophysical analysis of mechano-electrical transduction. In *Handbook of Sensory Physiology. I. Principles of Receptor Physiology*, ed. LOEWENSTEIN, W. R. Berlin, Heidelberg, New York: Springer-Verlag.

TERZUOLO, C. A. & WASHIZU, Y. (1962). Relation between stimulus strength, generator potential and impulse frequency in stretch receptor of Crustacea. *J. Neurophysiol.* **25**, 56–66.

WEIDMANN, S. (1951). Effect of current flow on the membrane potential of cardiac muscle. *J. Physiol.* **115**, 227–236.

WILSON, H. R. & COWAN, J. D. (1972). Excitatory and inhibitory interactions in localized populations of model neurons. *Biophys. J.* **12**, 1–24.

WINFREE, A. T. (1977). Phase control of neural pacemakers. *Science, N.Y.* **197**, 761–763.